RSC Advances

ROYAL SOCIETY OF CHEMISTRY

www.rsc.org/advances

Journal Name

ARTICLE

Pd nanoparticles modified rod-like nitrogen-doped ordered mesoporous carbons for effective catalytic hydrodechlorination of chlorophenols

Received 00th January 20xx,
Accepted 00th January 20xx

DOI: 10.1039/x0xx00000x

www.rsc.org/

Wei Zhang,[a] Fushan Wang,[b] Xinlin Li,[a] Yansheng Liu,[a] and Jiantai Ma*[, a]

The preparation of the rod-like nitrogen-doped ordered mesoporous carbons (NOMCs) through a facial aqueous soft-template self-assembly route in one-pot is presented in this work. After calcination at 800 °C under a nitrogen atmosphere, NOMCs with large specific surface area (~ 419.3 $m^2 g^{-1}$), high pore volume (~ 0.33 $cm^3 g^{-1}$), highly ordered mesostructure, and rich nitrogen content of 5.4 wt% were obtained. When NOMCs were used as the catalyst support, Pd nanoparticles (Pd NPs) could be well dispersed on the surface and in the mesopores, possibly owing to the coordination between the Pd NPs and the nitrogen atoms. And the Pd modified NOMCs nanocatalyst exhibited higher catalytic performance for the hydrodechlorination of chlorophenols under mild conditions, compared with other Pd supported catalysts.

Introduction

Chlorophenols (CPs), which are the important commercial industrial raw materials, have been widely applied in different domains. [1, 2] However, they have the characters of highly toxic, poorly degradable, bioaccumulative, which do harm to the environment. [2, 3] Therefore, many efforts have been made for the treatment of these pollutants. Among these processes, hydrodechlorination (HDC) is considered as the most effective way, because phenol is the single product and could be subsequently recycled. [2, 4-6] Thus, from the view of green chemistry, the development of new catalysts with high catalytic activity for one pot HDC of the CPs is highly desirable.

Among various carbon materials that can be used as catalyst supports, ordered mesoporous carbons (OMCs) have attracted a great deal of research. Considerable progress has been made in the design and controlled fabrication of OMCs with a defined morphology in the past decade due to their unique textural characteristics, for instance, ordered mesochannels, high surface area, and high pore volume. [7-9] These features are showing potentially advantageous in tremendous fields (e.g. catalysis, [10-12] sensing, [13] adsorption, [14-16] and energy storage/conversion [17, 18]). Meanwhile, incorporation of heteroatoms such as boron, nitrogen, oxygen, phosphorus and sulfur into OMCs has also been a burgeoning research topic, because substitutional doping of heteroatoms into carbon nanomaterials can further expand/enhance their properties for the increase of surface polarity and electron donor properties of the carbon materials; and introduce active catalytic sites to the carbon surface. [19-23] This is why heteroatom-doped carbon materials have become as more interesting materials than their un-doped materials for us in energy storage, catalysis and so on. [24] In particular, nitrogen-doped ordered mesoporpous carbons (NOMCs) are the most studied heteroatom-doped carbon materials. [24-27]

The common synthesis method of NOMCs is through a multistage nanocasting process (also known as the hard-template method) by utilizing appropriate nanosized mesoporous silica or silica spheres (SBA-15, FDU-12, KIT-6, MCM-41, MCM-48) as the hard template and nitrogen-containing sources as the carbon precursors, [24, 28-32] such as pyrrole, acrylonitrile, acetonitrile, aniline, dicyandiamide, melamine and N-containing ionic liquids. [24, 30-33] Though the incorporation of nitrogen into OMCs by the hard-template method is fairly well developed, it is still a great need for new strategy to synthesize NOMCs, because the hard-template method is inefficient, high in cost, time-consuming and environmentally harmful. Moreover, the morphologies and mesostructures of the NOMCs are limited by their front templates. [34] More recently, an organic-organic, soft-template direct synthetic approach via self-assembly of resins and amphiphilic block copolymers has brought a new strategy to synthesize NOMCs, providing new opportunities for various structures, morphologies and large-scale production. Compared with the hard-template method, the soft-template method needs fewer steps and has proven to be an effective way for the synthesis of OMCs or NOMCs. However, the soft-template method usually generates amorphous, monolithic or spherical mesoporous carbon nanomaterials. For example, Liu

[a] Gansu Provincial Engineering Laboratory for Chemical Catalysis, College of Chemistry and Chemical Engineering, Lanzhou University, Lanzhou 730000, PR China
[b] Lanzhou Petrochemical Company, PetroChina, Lanzhou 730060, PR China
E-mail addresses: majiantai@lzu.edu.cn (Jiantai Ma), Tel.: +86 0931 891 2577; Fax: +86 0931 891 2582

et al. developed a hydrothermal route via using resorcinol, hexamethylenetetramine (HMT), 1,3,5-trimethylbenzene (TMB) and F127 to synthesize monolithic OMCs; [35] Li *et al.* also developed a hydrothermal process to form sphere-like and rod-like OMCs by just changing the concentration of the morphological control agent F127, but it contains multistep procedures and is complicated. [36] Subsequently, Yang *et al.* introduced melamine to the organic aerogel precursors and formed the amorphous nitrogen-doped carbon aerogels; [37] Yu *et al.* used a similar synthesis procedure like Liu's method by add melamine to the reaction system and developed the monolithic NOMCs; [38] Wang *et al.* modified Liu's method by changing resorcinol to m-aminophenol (MAP) and successfully fabricated monolithic NOMCs. [27] Further on, they dissolved F127 in water to form micelles first and obtained the nitrogen-doped ordered mesoporpous carbon nanospheres. [39] Also, J. Tang *et.al* reported the synthesis of highly nitrogen-doped mesoporous carbon spheres with large mesopore sizes via a facile micelle route using the high-molecular-weight block polymer PS-b-PEO to form micelles as the template. [40] Consequently, the development to find simple, facile and practical methods to prepare NOMCs with defined morphology is still necessary.

Based on the abovementioned considerations, herein, we present a facial aqueous self-assembly route in one-pot for the synthesis of rod-like NOMCs. By simply adding suitable amount of ethanol into the solvent water, stirring with a moderate speed and carbonization, we prepared rod-like NOMCs. The NOMCs with high surface area, large pore volumes and nitrogen heteroatoms make them an applicable support candidate to form noble metal-based catalysts. We modified the NOMCs with Pd nanoparticles (Pd NPs) since the contained nitrogen heteroatoms (or nitrogen containing groups) could not only adsorb Pd^{2+} beneficially，but also stabilize Pd NPs to obtained well dispersed Pd NPs effectively. The application of Pd modified NOMCs (Pd/NOMCs) in the HDC of CPs was also demonstrated.

Experimental

Materials

Triblock copolymer Pluronic F127 (PEO106PPO70PEO106, Mw = 12600) was purchased from Energy Chemical (Shanghai). MAP, palladium acetate, 4-chlorophenol (4-CP) and other CPs were purchased from Shanghai Chemical Reagents Co., Ltd. Other chemicals were purchased from the Guangfu (Tianjin) Chemical Company. All chemicals were used as received without any further purification.

Preparation of the rod-like NOMCs

The NOMCs synthesis was prepared through modified procedures according to the reported literatures. [27, 35] Triblock copolymer (Pluronic F127) was used as a template, MAP used as the nitrogen-containing precursor, and HMT used as a slow release source of formaldehyde and then control the kinetics of the polymerization reaction. In a typical procedure, 2.0 g F127 and 0.48 g TMB were dissolved in deionized H_2O with adding suitable amount of ethanol, and stirred at room temperature for 1 h with a moderate speed. Then, 1.1 g MAP, 0.7 g HMT and 1.3 mL of 28 wt% aqueous ammonia were added to the above solution and the mixture was stirred at room temperature for another hour. Then, the solution was poured into a flask and transferred into an oil bath equipped with a water-cooled condenser at 80 ^{o}C stirred for 24 h. The as-made products (as-NOMCs) were collected by centrifugation, washed several times with water and ethanol and dried at 60 ^{o}C for 12 h in a vacuum oven. Finally, the as-NOMCs were calcined in a tubular furnace under a nitrogen atmosphere with the heating rate of 2 ^{o}C min^{-1} and kept the temperature at 800 ^{o}C for 3 h, then cooled to room temperature and finally the NOMCs were obtained.

Fabrication of the Pd/NOMCs nanocatalyst

The Pd/NOMCs nanocatalyst was prepared as follows: Firstly, NOMCs (200 mg) and 5 mL Pd acetate acetonitrile solution (2.0 mg mL^{-1}) were dispersed in a 10 mL round-bottom flask by ultrasound for 2 h, and stirred at room temperature for another 24 h. Then, the solid products were collected by removing the solvent acetonitrile using reduced pressure distillation and dried overnight in a vacuum oven at 40 ^{o}C. 200 mg of the above solid products were placed in a tubular furnace and reduced in a stream of H_2/N_2 (5%) at 250 ^{o}C for 2 h. The Pd/NOMCs nanocatalyst was obtained.

Procedure for the HDC of CPs

In a typical reaction, a certain amount of Pd/NOMCs nanocatalyst, 0.5 mmol of CPs and a certain amount of base (equimolar amount of Cl and sodium hydroxide) were added into the mixed solution of 20 mL H_2O. Prior to the reaction, a balloon filled with H_2 was connected to the flask, and the air in the flask was replaced by H_2 for at least three times. Then, the reaction was maintained at room temperature under vigorous stirring. To track the reaction progress, the reaction mixture was collected with a syringe at a certain time interval, and filtered through membrane filter, the filtrate was extracted by $CH_3COOC_2H_5$, and the results of the experiments were evaluated by GC–MS.

To study the reusability of the Pd/NOMCs nanocatalyst, after each HDC reaction, Pd/NOMCs nanocatalyst was recovered by centrifugation and then washed with water and dried in vacuum at room temperature for the next catalytic run.

Characterization

The morphology and the energy dispersive spectrometer (EDS) of the samples were performed on transmission electron microscope (TEM, JEOL 2010). Scanning electron microscope (SEM) images were taken using JSM-6701F field emission scanning electron microscope. Powder X-ray diffraction (XRD) patterns were recorded on a Rigaku D/max 2400 PC X-ray diffractometer using Cu Kα radiation in the 2θ range of 10–90°.

X-ray photoelectron spectroscopy (XPS, Perkin-Elmer PHI-5702) was used to analyse the surface electronic properties of the samples. The Brunauer–Emmett–Teller (BET) surface area and pore-size distribution are obtained by measuring N_2 adsorption isotherms at 77 K using a TriStar 3020 (Micromeritics). Elemental analysis was performed on a PerkinElmer EA2400 II instrument to determine the C, N content of the samples. Pd content of the prepared Pd/NOMCs nanocatalyst was obtained by inductively coupled plasma atomic emission spectroscopy (ICP–AES). The conversion of the reaction was estimated by using GC–MS (Agilent 5977E).

Results and discussion

Catalyst characterization

The rod-like NOMCs were fabricated via the soft-template method in one-pot as illustrated in Scheme 1. Then the NOMCs were ultrasonically dispersed in an acetonitrile solution containing Pd^{2+}, followed by reducing the adsorbed Pd^{2+} by H_2, and finally Pd/NOMCs nanocatalyst was obtained.

The morphology of the prepared materials NOMCs and Pd/NOMCs was characterized by SEM and TEM. As illustrated in SEM image Fig. 1a, the as-NOMCs with mostly rod-like morphology are presented. The TEM images (Fig. 1b, 1c) illustrates that the rod-like NOMCs have highly ordered mesostructures, and the width of the rod-like NOMCs is about 150-200 nm and the pore size is about 3 nm. Fig. 1d, 1e present the morphology of the Pd/NOMCs nanocatalyst. The Pd/NOMCs nanocatalyst was prepared by the impregnation–reduction method, the Pd NPs were not only dispersed on the surface but also wrapped in the mesopores of the rod-like NOMCs. The HRTEM image of Pd/NOMCs reveals that the particle size of the Pd NPs is about 3-5 nm (Fig. 1f). The inset picture of Fig. 1f also shows the lattice fringes of the Pd (1 1 1) planes (d = 0.23 nm) which attributes to the face-centered-cubic (fcc) Pd nanocrystals.

Small-angle XRD is a good method to describe the order of mesostructures. Fig. 2a reveals the small-angle XRD patterns of the NOMCs and Pd/NOMCs samples. Though the small-angle XRD pattern of the NOMCs shows only one peak and can be indexed as (1 0 0) reflection [27], it could also suggests the existence of the ordered mesostructures. The small-angle XRD pattern of the Pd/NOMCs has a very weak peak, we propose that it may be attributed to Pd NPs that are dispersed on the surface and wrapped in the mesopores of the NOMCs, so the ordered mesostructures of the NOMCs might be destroyed in a certain degree. [41]

Scheme 1. Fabrication procedure of the Pd/NOMCs.

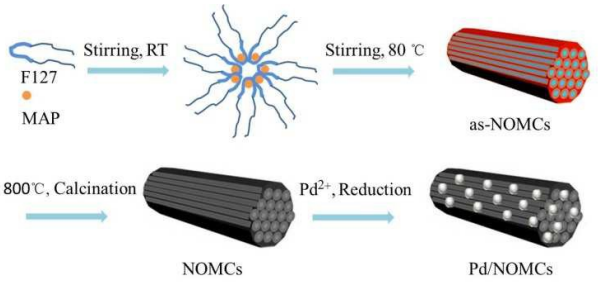

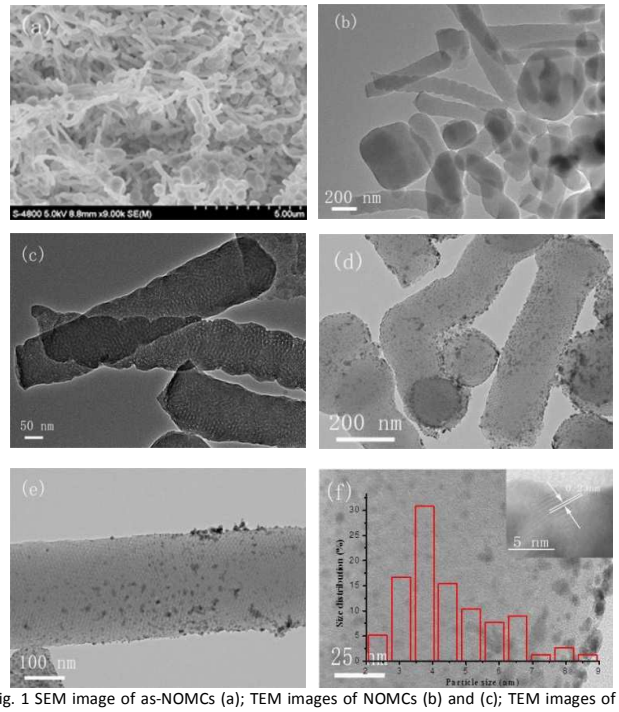

Fig. 1 SEM image of as-NOMCs (a); TEM images of NOMCs (b) and (c); TEM images of Pd/NOMCs (d) and (e); HRTEM of Pd/NOMCs (f), the inset shows the lattice of Pd and the Pd particle size distribution.

The wide-angle XRD analysis patterns of the samples NOMCs and Pd/NOMCs are presented in Fig. 2b. The NOMCs and Pd/NOMCs show two broad diffraction peaks with 2θ around 24° and 44°, which can be ascribed to the (0 0 2) plane of amorphous carbon and (1 0 0) plane of glassy carbon layers. [42, 43] In the XRD patterns of the Pd/NOMCs, it shows five peaks at around 40°, 46°, 67°, 81° and 85°, corresponding to the (1 1 1), (2 0 0), (2 2 0), (3 1 1) and (2 2 2) planes, which shows the typical fcc pattern of crystalline Pd particles (JCPDS-46-1043). [44] The EDS analysis was used to measure the chemical composition of NOMCs and Fig. 2c reveals the peaks corresponding to C, N and O indicating the nitrogen-doped carbons. The peak of copper (Cu) arises from Cu grid in TEM analysis. The nitrogen maintained at high temperature (800 ^{o}C) is mainly because its stable forms, namely, pyridinic, pyrrolic, graphitic and oxidized nitrogen (see XPS spectra below). And the contained nitrogen atoms help the immobilizition and prevent the leaching of Pd NPs.

XPS spectra were employed to confirm the chemical properties of the fabricated Pd/NOMCs. Fig. 3a shows clear signals from C, N, O and Pd, suggesting that N could be imported into the matrix via polymerization and Pd NPs are well supported on NOMCs. The C 1s spectrum of the Pd/NOMCs (Fig. 3b) could be deconvoluted into three single peaks centred at ~284.6, 285.8 and 286.5 eV, respectively. The strongest signal at ~284.6 eV is due to C–C bonding in a pure carbon environment of amorphous or graphitic carbon. The

peak at ~285.5 eV and 286.7 can be associated with the structure of C–N and C–O functionalities. [34, 39] The N 1s

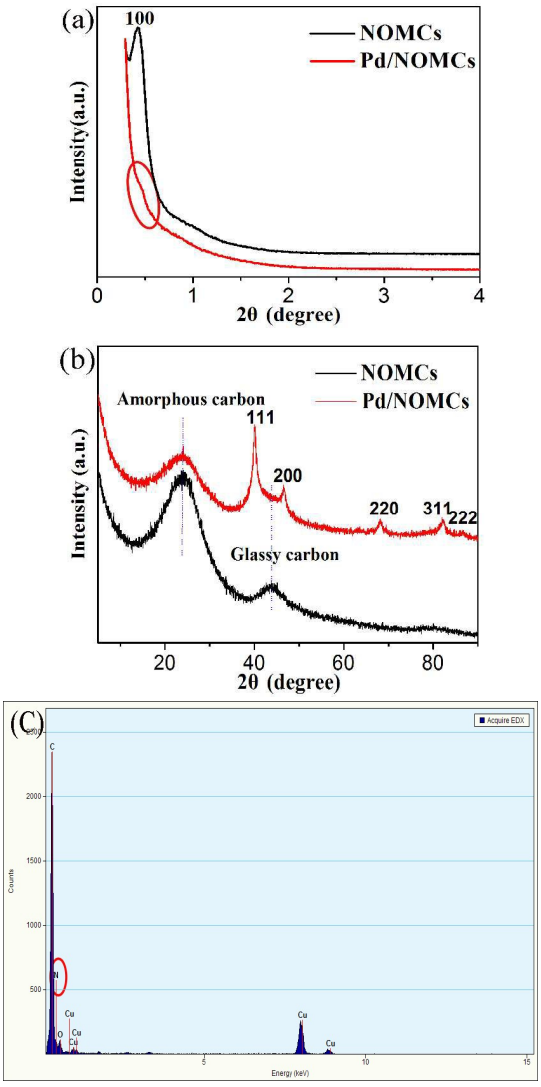

Fig. 2 Small-angle XRD patterns of NOMCs and Pd/NOMCs (a); wide-angle XRD patterns of NOMCs and Pd/NOMCs (b); EDS spectrum of NOMCs (c).

spectrum (Fig. 3c) can be fitted into four peaks with binding energies of ~398.2, 400.4, 401.0 and 402.6 eV, corresponding to pyridinic-N, pyrrolic-N, graphitic-N and oxidized-N, respectively. [25, 34, 39] The spectrum of O 1s of Pd/NOMCs (Fig. 3d) can be deconvoluted into three single peaks with binding energies of ~531.4, 532.6 and 533.8 eV that correspond to quinone, C=O, and C–OH, respectively.[45]

The Pd status of Pd/NOMCs is also determined by XPS, as shown in Fig. 3e, it is found that the ratio of Pd^0 is as high as 57.5% and the ratio of the Pd^{2+} is 42.5%, the existence of Pd^{2+} may mainly because the coordination between Pd^{2+} and the nitrogen groups on the surface of the NOMCs. Moreover, the weight percentage of Pd loading acquired from ICP-AES measurement is listed in Table 1. There is about 4.3 wt% of Pd in Pd/NOMCs. The N content obtained from elemental analysis is 5.4 wt%, it shows that N was successfully doped into the carbons. [32, 46]

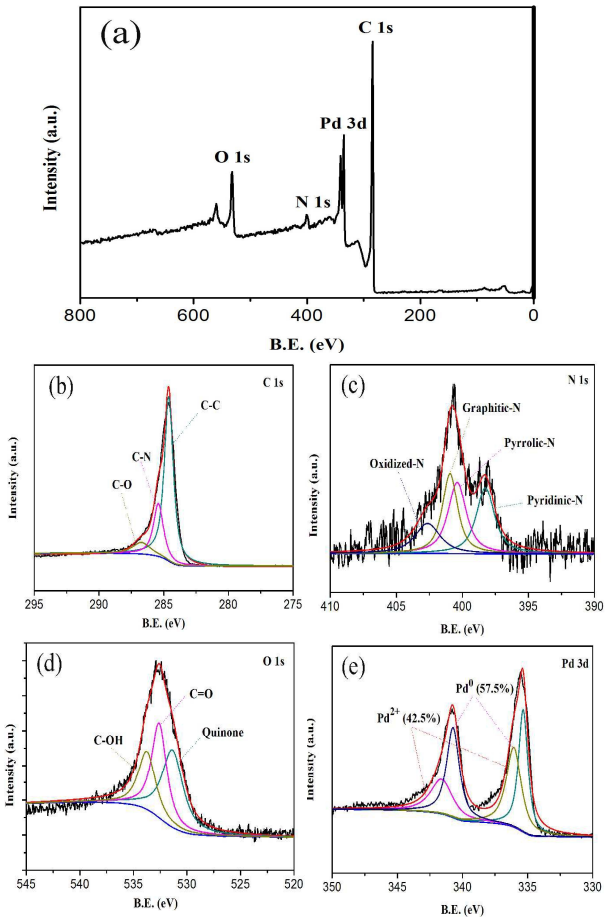

Fig. 3 XPS wide-scan spectrum of the Pd/NOMCs (a) and the C1s (b), N1s (c), O1s (d) and Pd 3d (e) spectra.

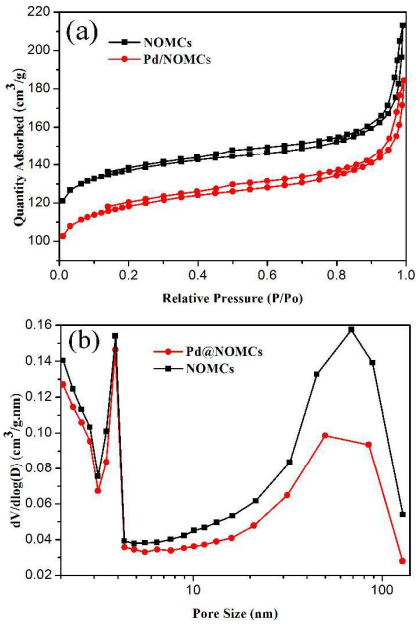

Fig. 4 Nitrogen adsorption–desorption isotherms (a) and pore size distribution (b) of NOMCs and Pd/NOMCs

Table 1 Textural parameters and elements content of the prepared samples

Samples	S_{BET}(m^2 g^{-1})	V_{pore}(cm^3 g^{-1})	D_{pore} (nm)	N (wt%)	C (wt%)	Pd (wt%)
NOMCs	419.3	0.33	3.14	5.4	89.8	
Pd/NOMCs	363.9	0.29	3.13			4.3
Pd/NOMCs[a]						4.1

[a] Pd/NOMCs nanocatalyst was measured after five successive runs of catalytic HDC of 4-CP.

Typical N_2 adsorption-desorption isotherms and corresponding pore size distribution of the NOMCs and Pd/NOMCs are given in Fig. 4. A hysteresis loop in the P/P_0 = 0.4-0.8 range is obtained for the NOMCs and Pd/NOMCs, showing typical type-IV curves and suggesting a uniform mesopore. [27, 39] Besides, the hysteresis loop at high relative pressures (P/P_0 > 0.9) confirmed the existence of some macropores, which might coming from the space of hollow cores. The pore size of the determined NOMCs based on the Barrett–Joyner–Halenda (BJH) pore-size distribution which was calculated from the desorption branches of the isotherms was about 3.14 nm; the Pd/NOMCs pore size was about the same as the NOMCs. The Brunauer–Emmett–Teller (BET) surface areas and pore volumes of the NOMCs and Pd/NOMCs are 419.3 m^2 g^{-1}, 0.33 cm^3 g^{-1} and 363.9 m^2 g^{-1}, 0.29 cm^3 g^{-1}, respectively (Table 1). Overall, the Pd NPs were successfully incorporated into the mesopores and dispersed on the surface of the rod-like NOMCs.

HDC experiments

Pd NPs based catalysts, as is well known, have excellent catalytic effect for the HDC of CPs. [32, 47] Therefore, the catalytic effect of Pd/NOMCs nanocatalyst is established by the HDC of CPs. The HDC of CPs is negligible without catalyst or in the presence of pure NOMCs at the same reaction conditions, which reveals that Pd NPs is indispensable for high catalytic activity.

The path way of the 4-CP HDC reaction is described as below: firstly, H_2 was adsorbed on the surface by the Pd NPs and then dissociated into two active hydrogen atoms. The C–Cl bond of the adsorbed 4-CP on the surface of the catalyst was attacked by the active hydrogen atom to form phenol and afford HCl. [48, 49] As HCl is a by-product and can poison catalysts, according to the previously reported works, for the HDC reaction in aqueous solution, NaOH was chosen as the best base to neutralize the HCl that generated during the HDC process. [1, 32] Firstly, the HDC of 4-CP was studied by using different catalyst dosage. The time evolution of the conversion of 4-CP and the yield of phenol with 10 mg, 20 mg and 40 mg Pd/NOMCs nanocatalysts were shown in Fig. 5a–c. From which, it could be seen that the greater the catalyst dosage is, the higher the catalytic activity is, because the high concentration of catalyst introduced more active sites and subsequently enhanced the catalytic activity. [47]

In the catalyzed HDC reaction, H_2 was in excessive amount in compare with 4-CP and can be supposed as constant during

Table 2 Catalytic HDC and further hydrogenation of different CPs over the Pd/NOMCs nanocatalyst.

Substrates	Catalyst dosage (mg)	Phenol Time(min)/Yield%	CYC Time(h)/Yield%
4-CP	10	60/97.8	24/2.1
4-CP	20	40/99.6	24/7.0
4-CP	40	30/99.5	24/11.6
2-CP	20	60/99.8	24/5.1
3-CP	20	60/99.9	24/10.6
2,4-DCP	20	90/97.1	24/12.1
2,4,6-TCP	20	120/96.6	24/10.8

All reactions were performed at ambient temperature with 1 atm H_2.

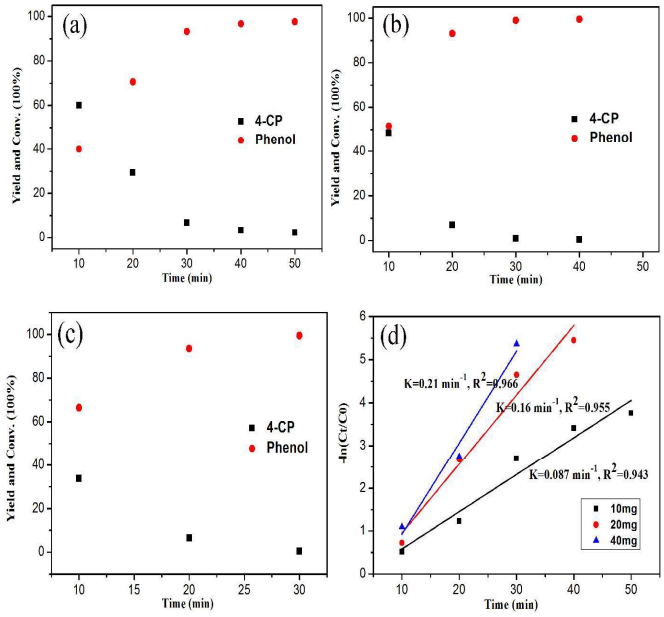

Fig. 5 Time evolution of the conversion of 4-CP and yield of phenol over different amounts of Pd/NOMCs nanocatalyst (these three reactions were performed at the same time). (a) 10 mg (Pd, 0.81 mol% to 4-CP), (b) 20 mg (Pd, 1.61 mol% to 4-CP) and (c) 40 mg (Pd, 3.23 mol% to 4-CP). (d) Plots of $-\ln(C_t/C_0)$ versus reaction time for the HDC of 4-CP over different amounts of Pd/NOMCs nanocatalyst.

the reaction time; therefore, the rate constant for the HDC of 4-CP followed the first-order kinetics. Using the reaction kinetics $-\ln(C_t/C_0) = kt$, the reaction rate constants were calculated to be 0.087 min^{-1}, 0.160 min^{-1} and 0.210 min^{-1}, respectively, for the HDC of 4-CP catalyzed by 10 mg, 20 mg and 40 mg Pd/NOMCs nanocatalyst (Fig. 5d). We found 20 mg of catalyst dosage in the reaction rate was about 2 times of 10 mg, but 40 mg of catalyst dosage was not 2 times of the 20 mg. We proposed that it because when the catalyst dosage was 40mg, the reaction active sites were excessive that not all the active sites were involved in the reaction. The reaction rate constant per unit mass $k_0 = k/M_{Pd}$ was calculated to be 202.3 min^{-1} g^{-1} for HDC of 4-CP catalyzed by 10 mg Pd/NOMCs, while for the previously reported Pd/pillared clays catalyst and the Pd/Al_2O_3 catalyst, the k_0 are 7.60 min^{-1} g^{-1} and 3.33 min^{-1} g^{-1},

respectively. [49, 50] Therefore, the Pd/NOMCs showed higher catalytic activity in the HDC of 4-CP.

In order to use the catalyst efficiently and economically, we chose the catalyst dosage 20 mg to perform the catalytic HDC

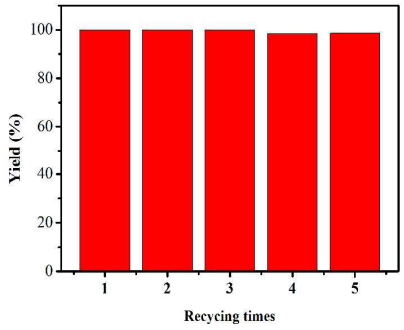

Fig. 6 The reusability of Pd/NOMCs nanocatalyst for catalytic HDC of 4-CP.

of other substituted CPs. At the same reaction conditions, all the other CPs such as 2-CP, 3-CP, 2,4-DCP and 2,4,6-TCP can also almost completely dechlorination. Thus, it indicates that Pd/NOMCs also have good activity for a wide range of substrates. Interestingly, as the HDC reaction proceeded, a small amount of cyclohexanone (CYC) begins to generate. This phenomenon is in agreement with other researchers' works [32, 51]. When the reaction time was lengthened to 24 hours, the results are presented in Table 2.

Furthermore, the circulation experiment of the catalyst was also investigated by using 20 mg Pd/NOMCs for the catalytic HDC of 4-CP (Fig. 6). The catalyst is reclaimed by centrifugation with simple decantation of the liquid products, washed with deionized water, and dried in vacuo at ambient temperature for the next catalytic run without further purification. It showed the yield of phenol remained at high levels even after five successive runs. And after 5 recycling times, the metal loading of Pd/NOMCs catalyst is still remains at 4.1% instead of the original 4.3% (Table 1). This result confirmed the stability and recyclability of the Pd/NOMCs. It also showed that the contained nitrogen heteroatoms served as coordination sites could stabilize the Pd NPs beneficially.

Conclusions

In summary, rod-like NOMCs have been successfully prepared through a facile aqueous soft-template self-assembly approach. As support, owing to the contained nitrogen heteroatoms which served as coordination sites, Pd NPs could be well dispersed on the surface and in the mesopores. The Pd/NOMCs nanocatalyst was applied as a heterogeneous catalyst for the HDC of CPs under mild conditions and showed excellent catalytic performance. And with the increase of the reaction time, a tiny amount of CYC was generated. Thus, the Pd/NOMCs as a relatively green, environmental friendly, and economical catalyst shows potential application in the HDC of CPs leading to their environmental sustainability disposal and could have good potential applications in various fields.

Acknowledgements

The authors acknowledge financial support from the Fundamental Research Funds for the Central Universities (lzujbky-2015-21 and lzujbky-2015-32).

Notes and references

1. Z. Dong, X. Le, C. Dong, W. Zhang, X. Li and J. Ma, *Appl. Catal. B: Environ.*, 2015, **162**, 372-380.
2. C. Xia, Y. Liu, S. Zhou, C. Yang, S. Liu, J. Xu, J. Yu, J. Chen and X. Liang, *J. Hazard. Mater.*, 2009, **169**, 1029-1033.
3. S. Sen Gupta, M. Stadler, C. A. Noser, A. Ghosh, B. Steinhoff, D. Lenoir, C. P. Horwitz, K. W. Schramm and T. J. Collins, *Science*, 2002, **296**, 326-328.
4. L. Calvo, A. F. Mohedano, J. A. Casas, M. A. Gilarranz and J. J. Rodríguez, *Carbon*, 2004, **42**, 1377-1381.
5. J. B. Hoke, G. A. Gramiccioni and E. N. Balko, *Appl. Catal. B: Environ.*, 1992, **1**, 285-296.
6. L. Calvo, M. A. Gilarranz, J. A. Casas, A. F. Mohedano and J. J. Rodríguez, *Appl. Catal. B: Environ.*, 2006, **67**, 68-76.
7. W. Shen and W. Fan, *J. Mater. Chem. A*, 2013, **1**, 999-1013.
8. T. Y. Ma, L. Liu and Z. Y. Yuan, *Chem. Soc. Rev.*, 2013, **42**, 3977-4003.
9. C. Liang, Z. Li and S. Dai, *Angew. Chem. Int. Ed.*, 2008, **47**, 3696-3717.
10. X. Xu, M. Tang, M. Li, H. Li and Y. Wang, *ACS Catal.*, 2014, **4**, 3132-3135.
11. L. Guo, W.-J. Jiang, Y. Zhang, J.-S. Hu, Z.-D. Wei and L.-J. Wan, *ACS Catal.*, 2015, 2903-2909.
12. R. Liu, D. Wu, X. Feng and K. Müllen, *Angew. Chem. Int. Ed.*, 2010, **49**, 2565-2569.
13. E. Z. Lee, Y.-S. Jun, W. H. Hong, A. Thomas and M. M. Jin, *Angew. Chem. Int. Ed.*, 2010, **49**, 9706-9710.
14. Z. Wu and D. Zhao, *Chem. Commun.*, 2011, **47**, 3332-3338.
15. Y. Xia, R. Mokaya, G. S. Walker and Y. Zhu, *Adv. Energy. Mater.*, 2011, **1**, 678-683.
16. A. Chen, C. Liu, Y. Yu, Y. Hu, H. Lv, Y. Zhang, S. Shen and J. Zhang, *J. Hazard. Mater.*, 2014, **276**, 192-199.
17. J. Wang, H. L. Xin and D. Wang, *Part. Part. Syst. Char.*, 2014, **31**, 515-539.
18. Y. Zhai, Y. Dou, D. Zhao, P. F. Fulvio, R. T. Mayes and S. Dai, *Adv. Mater.*, 2011, **23**, 4828-4850.
19. X. Wang, R. Liu, M. M. Waje, Z. Chen, Y. Yan, K. N. Bozhilov and P. Feng, *Chem. Mater.*, 2007, **19**, 2395-2397.
20. Y. Chang, F. Hong, J. Liu, M. Xie, Q. Zhang, C. He, H. Niu and J. Liu, *Carbon*, 2015, **87**, 424-433.
21. J. Jiang, H. Chen, Z. Wang, L. Bao, Y. Qiang, S. Guan and J. Chen, *J. Colloid Interface Sci.*, 2015, **452**, 54-61.
22. W. Kim, M. Y. Kang, J. B. Joo, N. D. Kim, I. K. Song, P. Kim, J. R. Yoon and J. Yi, *J. Power Sources*, 2010, **195**, 2125-2129.
23. J. Zhou, K. Wu, W. Wang, Z. Xu, H. Wan and S. Zheng, *Appl. Catal. A: Gen.*, 2014, **470**, 336-343.
24. V. C. Almeida, R. Silva, M. Acerce, O. P. Junior, A. L. Cazetta, A. C. Martins, X. Huang, M. Chhowalla and T. Asefa, *J. Mater. Chem. A*, 2014, **2**, 15181-15190.
25. X. Wang, C.-G. Liu, D. Neff, P. F. Fulvio, R. T. Mayes, A. Zhamu, Q. Fang, G. Chen, H. M. Meyer, B. Z. Jang and S. Dai, *J. Mater. Chem. A*, 2013, **1**, 7920-7926.
26. W. Li, D. Chen, Z. Li, Y. Shi, Y. Wan, G. Wang, Z. Jiang and D. Zhao, *Carbon*, 2007, **45**, 1757-1763.

27. J. Wang, H. Liu, X. Gu, H. Wang and D. S. Su, *Chem. Commun.*, 2014, **50**, 9182-9184.
28. N. Liu, L. Yin, C. Wang, L. Zhang, N. Lun, D. Xiang, Y. Qi and R. Gao, *Carbon*, 2010, **48**, 3579-3591.
29. M. Kruk, M. Jaroniec, R. Ryoo and S. H. Joo, *J. Phys. Chem. B*, 2000, **104**, 7960-7968.
30. J. Xu, T. Chen, Q. Jiang and Y.-X. Li, *Chemistry – An Asian Journal*, 2014, **9**, 3269-3277.
31. Z. Zhao, Y. Dai, J. Lin and G. Wang, *Chem. Mater.*, 2014, **26**, 3151-3161.
32. Z. Dong, C. Dong, Y. Liu, X. Le, Z. Jin and J. Ma, *Chem. Eng. J.*, 2015, **270**, 215-222.
33. X. Xu, H. Li and Y. Wang, *ChemCatChem*, 2014, **6**, 3328-3332.
34. Z. Wu, P. A. Webley and D. Zhao, *J. Mater. Chem.*, 2012, **22**, 11379-11389.
35. D. Liu, J.-H. Lei, L.-P. Guo, D. Qu, Y. Li and B.-L. Su, *Carbon*, 2012, **50**, 476-487.
36. M. Li and J. Xue, *J. Colloid Interface Sci.*, 2012, **377**, 169-175.
37. Y. Yang, B. Zhao, P. Tang, Z. Cao, M. Huang and S. Tan, *Carbon*, 2014, **77**, 113-121.
38. J. Yu, M. Guo, F. Muhammad, A. Wang, G. Yu, H. Ma and G. Zhu, *Micropor. Mesopor. Mater.*, 2014, **190**, 117-127.
39. J. Wang, H. Liu, J. Diao, X. Gu, H. Wang, J. Rong, B. Zong and D. S. Su, *J. Mater. Chem. A*, 2015, **3**, 2305-2313.
40. J. Tang, J. Liu, C. Li, Y. Li, M. O. Tade, S. Dai and Y. Yamauchi, *Angew. Chem. Int. Ed.*, 2015, **54**, 588-593.
41. Z. Li, J. Liu, C. Xia and F. Li, *ACS Catal.*, 2013, **3**, 2440-2448.
42. J.-C. Song, Z.-Y. Lu and Z.-Y. Sun, *J. Colloid Interface Sci.*, 2014, **431**, 132-138.
43. H. R. Choi, H. Woo, S. Jang, J. Y. Cheon, C. Kim, J. Park, K. H. Park and S. H. Joo, *ChemCatChem*, 2012, **4**, 1587-1594.
44. H. A. Elazab, A. R. Siamaki, S. Moussa, B. F. Gupton and M. S. El-Shall, *Appl. Catal. A: Gen.*, 2015, **491**, 58-69.
45. X. Zhao, Q. Zhang, B. Zhang, C.-M. Chen, A. Wang, T. Zhang and D. S. Su, *J. Mater. Chem.*, 2012, **22**, 4963-4969.
46. X. Liu, Z. Zhang, Y. Yang, D. Yin, S. Su, D. Lei and J. Yang, *Chem. Eng. J.*, 2015, **263**, 290-298.
47. B. Yang, S. Deng, G. Yu, Y. Lu, H. Zhang, J. Xiao, G. Chen, X. Cheng and L. Shi, *Chem. Eng. J.*, 2013, **219**, 492-498.
48. S. Wang, B. Yang, T. Zhang, G. Yu, S. Deng and J. Huang, *Ind. Eng. Chem. Res.*, 2010, **49**, 4561-4565.
49. E. Díaz, J. A. Casas, Á. F. Mohedano, L. Calvo, M. A. Gilarranz and J. J. Rodríguez, *Ind. Eng. Chem. Res.*, 2008, **47**, 3840-3846.
50. C. B. Molina, A. H. Pizarro, J. A. Casas and J. J. Rodriguez, *Appl. Catal. B: Environ.*, 2014, **148–149**, 330-338.
51. Y. Liu, Z. Dong, X. Li, X. Le, W. Zhang and J. Ma, *Rsc Adv.*, 2015, **5**, 20716-20723.